

IMAGE LICENSED BY INGRAM PUBLISHING

FERROELECTRIC DEVICES HAVE gained significant interest, owing to their diverse range of applications in fields such as non-volatile memories, steep-slope transistors, neuromorphic and in-memory computing. Accurate modeling of ferroelectric devices is crucial to optimize these devices for different applications and design high-performance circuits. This article presents an overview of the current state of ferroelectric modeling at material, device, and circuit levels. We examine the unique aspects and limitations of the current modeling techniques and highlight potential areas of further research to advance this field.

# Material, Device and Circuit-Compatible Modeling of Ferroelectric Devices

An Overview

Digital Object Identifier 10.1109/MNANO.2023.3278970  
Date of current version: 19 July 2023

REVANTH KODURU, TANMOY KUMAR PAUL, AND SUMEET KUMAR GUPTA

## INTRODUCTION

Ferroelectric materials, owing to their non-centrosymmetric crystal structures, exhibit spontaneous polarization in the absence of external electrical fields. These non-zero remanent polarization states ( $\pm P_R$ ) can be switched from one to another by applying an electric field exceeding the coercive field ( $E_c$ ) of the material. This results in hysteretic polarization versus electric field (P-E) behavior, characteristic of ferroelectric (FE) materials as shown in Figure 1(a). The concept of ferroelectricity was first theorized by Erwin Schrodinger in 1912 and later discovered in Potassium Sodium Tartrate (or Rochelle salt) by Valasek in 1920 [1]. Subsequently, ferroelectric properties were discovered in another hydrogen-bonded material, Potassium Dihydrogen Phosphate (KDP). However, the fragility and water-solubility of these materials hindered the exploration of applications and understanding of ferroelectricity.

The discovery of ferroelectricity in bulk inorganic materials, such as perovskite-structured Barium Titanate ( $\text{BaTiO}_3$  – BTO) and Lead Zirconate Titanate ( $\text{PbZr}_x\text{Ti}_{1-x}\text{O}_3$  – PZT) in the 1940s and 50s, transformed the field of ferroelectrics [2]. These materials opened new avenues for ferroelectric applications, such as nonvolatile memories [3]. Further, the simple structure of BTO (Figure 1(b)) promoted investigations into the physical origins of ferroelectricity, and paraelectric-ferroelectric phase transitions around the Curie temperature ( $T_C$ ).

In the paraelectric phase above  $T_C$ ,  $\text{BaTiO}_3$  exhibits a cubic lattice (Figure 1(b)), where Ba atoms occupy the corners with the Ti atom at the body center and six oxygen atoms at the face centers. Below  $T_C$ ,  $\text{BaTiO}_3$  undergoes a ferroelectric phase transition into a tetragonal lattice with an elongated c-axis. In the FE phase, the Ti atom is displaced from its central position along the z-direction, resulting in two stable polarization states – corresponding to its upward and downward displacement from the centrosymmetric position. This structure of BTO prompted Devonshire to formulate a phenomenological model

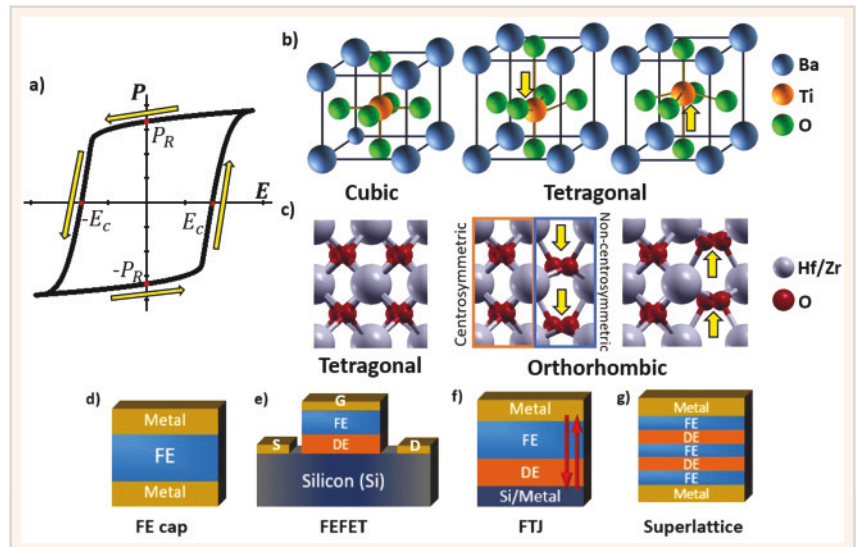


**FIGURE 1** (a) Hysteretic polarization ( $P$ ) versus electric-field ( $E$ ) curve of ferroelectric material. (b) Unit cell lattices for  $\text{BaTiO}_3$  in cubic and tetragonal phases showing the stable positions of Ti atom with downward and upward displacements from the center resulting in the spontaneous polarization. (c) Unit cell lattice of Zr-doped  $\text{HfO}_2$  (HZO) in tetragonal and the polar orthorhombic o111 phases, highlighting the centrosymmetric and non-centrosymmetric oxygen atoms along with the stable polarization states. Ferroelectric device structures (d) ferroelectric capacitor, (e) ferroelectric field effect transistor (FEFET), (f) metal-ferroelectric-insulator-semiconductor (MFIS) ferroelectric tunneling junction (FTJ) with tunneling currents and (g) ferroelectric-dielectric superlattice structures.

of ferroelectricity, in which the free energy of the ferroelectric material is modeled as a double-well potential [4]. This model will be discussed in more detail in the subsequent section.

In 1984, the stabilization of ferroelectricity in thin films marked a significant breakthrough in this field, reducing the switching voltages from hundreds of volts to tens of volts. This advancement enabled the development of FE capacitors (Figure 1(d)) and facilitated the integration of ferroelectrics with semiconductors, resulting in the realization of Ferroelectric Field Effect Transistors (FEFETs) (Figure 1(e)) [5]. Additionally, FE thin films led to the realization of a novel device – Ferroelectric Tunnel Junction (FTJ) (Figure 1(f)). FTJ is based on the concept of polarization-dependent tunneling current or Tunneling Electro-Resistance (TER), as proposed by Esaki [6]. These developments played a crucial role in commercializing ferroelectric-based devices in non-volatile memories and Ferroelectric Random-Access Memories (FERAMs) [3].

However, the commercial success of ferroelectric devices in integrated elec-

tronics was limited due to several challenges [3], [7]. Devices based on PZT, and other perovskite ferroelectrics suffered from polarization fatigue. Several attempts were made to overcome this problem, such as the development of superlattice structures (Figure 1(g)) – Strontium Bismuth Tantalate (SBT). However, the complex structure of superlattices coupled with the weakly bonded oxygen atoms in perovskite materials posed challenges for their CMOS process integration [3]. Additionally, the poor scalability of perovskite-based FERAMs and the small bandgap of perovskites restricted their widespread adoption in scaled electronics [3].

The discovery of ferroelectricity in Hafnium-Oxide ( $\text{HfO}_2$ ) doped with Si in 2011 [8] and subsequently with Zr and other tri and tetra valent atoms marked a major milestone in the field of ferroelectrics. Unlike perovskites, ferroelectric  $\text{HfO}_2$  exhibits a fluorite crystal structure with an orthorhombic lattice (Figure 1(c)). In this structure, the non-centrosymmetric oxygen atoms switch between two stable positions giving rise to spontaneous polarization. Prior to the

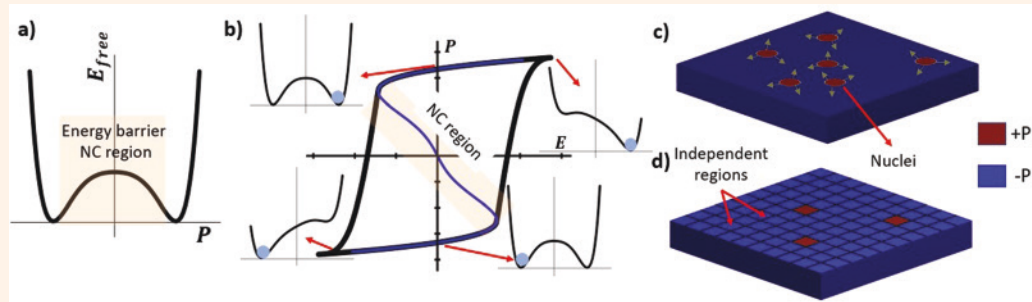


**FIGURE 2** (a) Landau free energy profile showing the stable polarization states and the energy barrier separating them. (b) Hysteretic polarization (P)- electric field (E) loop overlapped with the Landau curve, highlighting the negative capacitance region and the hysteretic behavior as the traversal of free energy landscape in the presence of electric field. (c) Polarization profile of the ferroelectric layer showing the nucleated domains and their growth as proposed by the KAI model. (d) Polarization profile of the ferroelectric layer divided into multiple independent regions according to NLS model, highlighting their independent switching behavior.

discovery of its ferroelectric properties, HfO<sub>2</sub> was widely used in the semiconductor industry as a high-k material in the gate stack of MOSFETs. Thereby, already well-established techniques for the integration of HfO<sub>2</sub> with the CMOS process renewed the interest in ferroelectric devices [7].

In addition to CMOS-process compatibility, HfO<sub>2</sub>-based FE devices exhibit various appealing attributes such as multi-level operation, stochastic switching, and polarization accumulation [7], [29], [30], [31], [32], [33]. By virtue of these attributes, HfO<sub>2</sub>-based FE devices are shown as promising candidates for various in-demand applications such as steep-switching transistors (NCFETs) [13], multi-level non-volatile memories, neuromorphic computing (as neurons and synapses) and in-memory computing [7]. Further, the large bandgap (>5eV) of HfO<sub>2</sub> coupled with its scale-free nature of ferroelectricity [9], as revealed by first-principles studies, make HfO<sub>2</sub> a highly promising material for advanced technology nodes and future electronics.

Despite these desirable properties, commercialization of HfO<sub>2</sub>-based FE devices faces certain challenges that need to be addressed. Some of the main challenges include device-to-device variability, and limited endurance (due to wake-up and fatigue effects) [7], [10]. These limitations arise from a variety of factors such as polycrystalline and polymorphic nature of HfO<sub>2</sub>, defects, and charge trapping. To address these challenges, a considerable amount of research

effort is being directed towards optimizing material properties of HfO<sub>2</sub> via process and material engineering techniques. In addition, development of superlattice structures combining HfO<sub>2</sub> with interlayer dielectrics and anti-ferroelectric ZrO<sub>2</sub> is being explored [7], [10].

Over the past century, ferroelectricity has been discovered in numerous materials, and various flavors of ferroelectric devices have been demonstrated as promising candidates for a wide range of applications. Throughout this journey, modeling of ferroelectric materials and devices has played a crucial role in advancing our fundamental understanding of ferroelectricity and its physical principles [11], [12], [13], [14], [15], [16], [17], [18], [19], [20], [21], [22], [23], [24], [25], [26], [27], [28], [29], [30], [31], [32], [33], [34], [35], [36], [37], [38], [39], [40], [41], [42], [43], [44], [45]. Modeling of ferroelectric materials has been pivotal in overcoming various challenges in perovskites and HfO<sub>2</sub> and optimizing their ferroelectric properties. Moreover, accurate modeling of ferroelectric devices has allowed for the correlation of device characteristics with the underlying material properties, as well as the exploration of diverse applications for ferroelectrics.

In the current state, where the field of ferroelectrics encompasses a broad range of materials and applications, modeling of ferroelectric materials and devices has become an indispensable tool in optimizing them for specific applications. Further, as we continue to push for bet-

ter performance, developing circuit-compatible models for FE devices has become increasingly important due to their significant role in driving circuit and architecture level optimizations. This article provides an overview of recent advancements in ferroelectric modeling at different levels of abstraction viz. material-level, device-level, and circuit-compatible models. These models, at different levels of detail, complement each other, providing a comprehensive understanding of device behavior at different scales.

Material-level models deal with atomistic simulations of ferroelectric materials, which help in understanding the intrinsic properties of FE materials and their dependence on process conditions. Device-level models incorporate material-level insights along with the device-level interactions and constraints to model and study the electrical characteristics of ferroelectric devices. On the other hand, circuit compatible models provide a simplified model for ferroelectric devices, trading accuracy for speed. These models are developed to be utilized in circuit-simulation software to evaluate the implications of FE device at circuit-level. Although, this article focusses on modeling of doped HfO<sub>2</sub> based devices and to some extent perovskites, the models reviewed here can be easily adapted to suit other materials.

## THEORIES OF FERROELECTRIC POLARIZATION SWITCHING

A fundamental understanding of polarization response to the external electric field is critical in accurately modeling

ferroelectric devices. Therefore, we will start with a brief overview on the theories of polarization switching. Over the years, several theories have been developed to explain the origins of ferroelectricity and capture the hysteretic characteristics. In this section, we will review a few of these theories that are widely used in modeling ferroelectric devices.

### LANDAU-GINZBURG-DEVONSHIRE (LGD) FORMALISM

The Landau-Devonshire theory [4], proposed by Devonshire in the 1950s, provides a phenomenological approach for understanding ferroelectric materials. This theory models the free energy of ferroelectric material as a double-well potential with an energy barrier separating the two stable polarization states (Figure 2(a)). Based on the symmetry consideration of the Landau theory of phase-transitions, the free energy ( $E_{free}$ ) is expanded as a polynomial of even terms in the polarization ( $P$ ).

$$\begin{aligned} E_{free} = & \alpha_1 (P_1^2 + P_2^2 + P_3^2) \\ & + \alpha_{11} (P_1^4 + P_2^4 + P_3^4) \\ & + \alpha_{111} (P_1^6 + P_2^6 + P_3^6) \\ & + \alpha_{12} (P_1^2 P_2^2 + P_2^2 P_3^2 + P_1^2 P_3^2) \\ & + \alpha_{112} (P_1^4 (P_2^2 + P_3^2) \\ & + P_2^4 (P_1^2 + P_3^2) \\ & + P_3^4 (P_1^2 + P_2^2) + \dots \end{aligned}$$

where  $P_1, P_2, P_3$  are polarization vectors in  $x, y, z$  directions and  $\alpha_1, \alpha_{11}, \alpha_{111}, \alpha_{12}, \alpha_{112}$  are material-specific parameters. These parameters are determined either by fitting the experimental results or from first-principles calculations. The temperature dependence of dielectric constant and ferroelectric properties, to first order, are captured by considering  $\alpha_1 = \alpha_0 (T - T_C)$ . Below the Curie temperature ( $T_C$ ),  $\alpha_1$  is negative and becomes positive above  $T_C$ , capturing the FE-paraelectric transition.

The equilibrium polarization state of the system is determined by minimizing the total energy of the system ( $F$ ) with respect to the polarization ( $P$ ) as

$$\frac{dF}{dP_i} = 0; i = 1, 2, 3$$

$$F = \iiint (E_{free} + E_{elec} + E_{elas} + E_{strict}) dV$$

$E_{elec}$  is the electrostatic energy of the FE material due to the electric field ( $E$ ) resulting from the applied potential and the improper screening of polarization charges at the ferroelectric interfaces (also known as depolarization field).

$$E_{elec} = -E \cdot P$$

In addition, the elastic ( $E_{elas}$ ) and electro-strictive ( $E_{strict}$ ) energies are sometimes considered to include the energy changes arising from the polarization-induced and external stress-induced structural distortions.

$$\begin{aligned} E_{elas} = & \frac{c_{11}}{2} (\eta_{11}^2 + \eta_{22}^2 + \eta_{33}^2) \\ & + c_{12} (\eta_{11} \eta_{22} + \eta_{22} \eta_{33} + \eta_{33} \eta_{11}) \\ & + 2c_{44} (\eta_{12}^2 + \eta_{23}^2 + \eta_{13}^2) \\ E_{strict} = & -\eta_{11} (\eta_{11} P_1^2 + \eta_{22} P_2^2 + \eta_{33} P_3^2) \\ & -\eta_{12} (\eta_{11} (P_2^2 + P_3^2) + \eta_{22} (P_1^2 + P_3^2) \\ & + \eta_{33} (P_1^2 + P_2^2)) - 2\eta_{44} (\eta_{12} (P_1 P_2) \\ & + \eta_{13} (P_1 P_3) + \eta_{23} (P_2 P_3)) \end{aligned}$$

Here,  $\eta_{ij}$  are the inhomogeneous stress components, calculated by solving the mechanical equilibrium equations.

The hysteretic behavior of ferroelectric materials can be understood as the transversal of polarization in response to the applied electric field in the free energy landscape (Figure 2(b)). However, the Landau-Devonshire (L-D) theory assumes that the polarization is homogeneous across the ferroelectric (FE) layer, which is rarely the case [11]. In practice, ferroelectrics often exhibit domain structures, where different regions have different polarizations. Domain formation can arise from various factors, such as underlying polycrystalline structure, defects, non-uniform strain, or simply to minimize the depolarization field and the associated electrostatic energy.

To account for the non-homogeneous nature of polarization in ferroelectrics, L-D theory has been extended by Ginzburg, resulting in the Landau-Ginzburg-Devonshire (LGD) theory [11]. The LGD theory includes the polarization

gradient energy ( $E_{grad}$ ) to the total energy, which accounts for the energy cost due to the non-uniform polarization.

$$E_{grad} = \frac{g_{ijkl}}{2} \frac{\partial P_i}{\partial x_j} \frac{\partial P_k}{\partial x_l} \quad i, j, k, l = 1, 2, 3$$

The LGD framework has been further extended to capture the dynamics of polarization switching through Time-dependent Ginzburg Landau (TDGL) equation. This equation determines the rate of polarization change as function of the thermodynamic force dependent on the energy of the system as

$$-\frac{1}{\Gamma} \frac{dP}{dt} = -\frac{dF}{dP}$$

The TDGL formalism provides a comprehensive approach for modeling the hysteretic and nonlinear behavior of ferroelectric materials. One of the advantages of using TDGL formalism is its ability to include various external perturbations, such as temperature and strain, and investigate their role on polarization switching [26], [27], [28], [29]. However, modeling FE devices using TDGL can be computationally intensive, and requires accurate determination of various material-specific parameters.

Additionally, TDGL formalism captures the non-hysteretic and hysteretic negative capacitance (NC) of the FE layer [12], arising due to the energy barrier (Figure 2(a)) separating the remanent polarization states. This negative capacitance can be stabilized by placing the FE layer in series with a dielectric layer, so that the total capacitance of the system is positive [12]. In 2008, Salahuddin et al. [13] proposed using this negative capacitance FE in the gate stack of a transistor to overcome the Boltzmann limit, which lead to the development of Negative Capacitance FETs (NCFETs). The modeling aspects of NCFETs at device level will be discussed in Section IV.

### KOLMOGOROV-AVRAMI-ISHIBASHI (KAI) MODEL

Ishibashi et al. developed the KAI model [14] to simulate the ferroelectric polarization switching dynamics in a computationally simpler manner. This semi-empirical model assumes that the

polarization switching is driven by the unrestricted growth of oppositely polarized domains, which are nucleated from different non-interacting nucleation sites (Figure 2(c)). When a switching electric field ( $E > E_C$ ) is applied, the kinetics of polarization is considered to be limited by the rate of growth and propagation of these opposite polarized domains.

Starting from a completely poled state (let's say  $-P_s$ ), the KAI model calculates the amount of polarization switched in the ferroelectric layer at any given time ( $t$ ) after the application of the switching electric field as

$$\Delta P = 2P_s \left( 1 - \exp\left(-\frac{t}{\tau}\right)^n \right)$$

Here,  $P_s$  is the saturation polarization,  $\tau$  is the characteristic time constant, which depends on the applied electric field and mobility of the domain walls in the ferroelectric material. The parameter  $n$  is the dimensionality of the nucleated domains.

The KAI model was successful in capturing the dynamics of polarization switching in bulk crystals and investigating the impact of various factors [15], [31]. However, its assumption of unrestricted growth of domains limits its applicability to FE thin films, especially for HfO<sub>2</sub>, due to the polycrystalline nature and the defects that hinder domain propagation [15]. Additionally, the KAI model assumes that a constant electric field is applied, and the ferroelectric layer is initially in a completely poled state, making it not universally applicable to all cases.

### NUCLEATION LIMITED SWITCHING (NLS) MODEL

To address the limitations of the KAI model, TagansteV et al. proposed the nucleation-limited switching (NLS) model [15]. The NLS model considers the FE layer to be composed of multiple independent regions, where the polarization switching is considered to be nucleation limited (Figure 2(d)). This is based on the understanding that the energy needed for the nucleation of oppositely polarized ( $+P$ ) domains is greater than the energy required for the propagation of these domains over the region.

As a result, when a switching electric field ( $E > E_C$ ) is applied, the polarization switching of a region is limited by the wait time for the nucleation of these oppositely polarized domains. The switching of a region ( $p$ ) by any given time ( $t$ ) is modeled as a Weibull process [14], [30], given by

$$p(t_s \leq t) = 1 - \exp\left(\left(-\frac{t}{\tau}\right)^\beta\right)$$

where the parameters  $\beta$  and  $\tau$  control the rate of nucleation. The characteristic time constant  $\tau$  depends on the local electric field ( $E$ ) and the activation field ( $E_a$ ) of the region as follows [30]:

$$\tau(E, E_a) = \tau_\infty \exp\left(\left(\frac{E}{E_a}\right)^\alpha\right)$$

To account for the variability in switching times across the regions, the activation field ( $E_a$ ) is considered to be randomly distributed as  $E_a = \eta E_{a0}$ , where  $\eta$  follows a probability density function,  $f(\eta)$ . Based on the switching probability of a region ( $p$ ) and the distribution of activation fields ( $E_a$ ), the polarization of the FE sample at any time ( $t$ ) is given by

$$P(t) = -P_s + 2P_s \int p(t_s \leq t | \tau(E, E_a), \beta) f(\eta) d\eta$$

The NLS model overcomes various limitations of the KAI model by restricting the domain propagation to the independent regions. The NLS model, as formulated above, still assumes that the ferroelectric layer is initially completely poled ( $-P_s$ ) and subjected to a constant electric field. However, various modifications have been proposed to the NLS model to account for arbitrary initial conditions and non-constant electric fields [31], [32], some of which will be discussed in Section IV.

### PREISACH MODEL OF HYSTERESIS

The Preisach model of hysteresis, originally developed for ferromagnetic materials, has been adapted to describe the hysteretic behavior of ferroelectric materials [16]. This theory considers that the ferroelectric layer is composed of independent dipoles or "hysteron" that switch when the electric field across them exceeds the coercive field ( $\pm E_c$ ). The

coercive field of the hysteron across the FE layer is considered to be randomly distributed. Thereby, the polarization of the FE layer for any given electric field is calculated by considering the fraction of hysteron that have switched. When the underlying coercive field distribution is assumed to be Gaussian, the dependence of polarization ( $P^\pm$ ) on the electric field ( $E$ ) can be described by hyperbolic tangent, as derived by Miller [17]:

$$\begin{aligned} P^\pm &= P_s \tanh\left(\frac{E \mp E_c}{2\delta}\right) \delta \\ &= E_c \ln\left(\frac{P_s + P_R}{P_s - P_R}\right)^{-1} \end{aligned}$$

Here,  $P_s$  is the saturation polarization,  $P_R$  is the remanent polarization and  $E_c$  is the mean coercive field of the FE layer.

However, the Preisach model assumes that the polarization can only point in two directions, making it difficult to capture the random polarization orientation in polycrystalline ferroelectrics. Moreover, the model neglects the dynamic aspects of polarization switching and assumes a large ensemble of dipoles in the FE layer, which may not hold true for highly scaled devices, limiting its applicability. Nonetheless, due to its analytical nature and lower computational requirements, the Preisach model was widely used in the early stages of ferroelectric device modeling and remains a popular choice for developing circuit compatible models [36], [43], [44].

### MATERIAL-LEVEL MODELS

A comprehensive understanding of the properties and the underlying physics of ferroelectric devices is essential for developing high-performance devices. Material-level models provide a means of studying ferroelectric devices at the atomistic scale, providing a detailed description of electronic and structural properties of the materials. They help establish correlations between various process parameters and the underlying material properties. This plays a significant role in driving the optimization strategies for ferroelectric fabrication and the development of superior-quality ferroelectric materials.

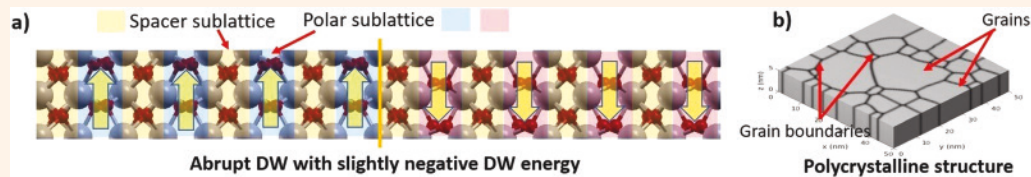


**FIGURE 3** (a) First principles simulations of HfO<sub>2</sub> showing the alternate spacer and polar layers with the sharp 180° domain wall. (b) Polycrystalline structure of HfO<sub>2</sub> showing the grains and grain boundaries.

Material-level modeling typically involves first-principles simulations based on the Density Functional Theory (DFT) and Molecular Dynamics (MD) calculations to simulate a small group of atoms [18]. The modern theory of polarization, proposed in 1993, formulating polarization as a Berry phase of the Bloch wave function was a turning point in making first-principles simulations the standard for material-level modeling of ferroelectric devices. In the journey of perovskite ferroelectrics, first-principles simulations were crucial in studying the various dependencies of polarization, extracting the TDGL parameters, understanding the domain walls and providing insights into the energy barriers for domain growth and nucleation [18]. Several articles have reviewed the impact of first-principles simulations on the theoretical breakthroughs in perovskites [18]. In this article, we will focus on how first-principles-based material-level models are driving the understanding and development of HfO<sub>2</sub>-based ferroelectrics.

Discovery of ferroelectricity in doped HfO<sub>2</sub> [8] surprised researchers as HfO<sub>2</sub> has been well established as a high-*k* material with only non-polar phases in its phase diagram. The most stable-phase at room temperature is the monoclinic (*m*-) phase, while the tetragonal (*t*-) and cubic (*c*-) phases are stabilized at high temperatures. Even with an increase in pressure, the most stable phases are the non-polar orthorhombic *oI* and *oII*. However, through theoretical [19], [20], [21], [26], and subsequent experimental works it was quickly established that the stabilization of the metastable polar orthorhombic *oIII* (*Pca2<sub>1</sub>*) phase is responsible for the ferroelectric properties of doped-HfO<sub>2</sub>.

The theoretical work of Materlik et al. [19] had been a significant contribution

in identifying the stability of *oIII* phase in ferroelectric HfO<sub>2</sub>. Their investigations into the energy landscape of various phases of Zr-doped HfO<sub>2</sub> (HZO) provided valuable insights into the interplay between surface and bulk free energies. The authors established the key role of polycrystalline grain size in stabilizing ferroelectricity in HfO<sub>2</sub>. Their study showed that under normal processing conditions, the *m*-phase of HfO<sub>2</sub> has the lowest bulk free energy, followed by *oIII* phase and *t*-phase. However, in polycrystalline thin films, determining the stability of phases requires considering both surface and bulk free energies. Materlik et al. [19] showed that the surface energy of *t*-phase is lower than the *oIII* phase, which, in turn, is lower than the *m*-phase. Thus, when the grains are large, the contribution of surface energy to the total energy is much lower than the bulk free energy and the *m*-phase is the most stable. However, as the grain size decreases, the surface energy becomes increasingly important, making the *oIII* phase stable. Finally, as the grains become too small, the *t*-phase dominates due to having the lowest surface energy of the three.

Continuing on this, many researchers have employed first principles simulations to provide deeper understanding of the critical factors in stabilizing the ferroelectric phase in HfO<sub>2</sub>. For instance, intermediate doping concentration ranges of various tri and tetra valent elements and slight oxygen-deficient conditions during fabrication have been shown to effectively stabilize the ferroelectric phase by limiting the grain sizes [20]. Additionally, these dopants and the oxygen vacancies are shown to stabilize the *t*-phase during annealing. This allows for a more kinetically favorable *t*-*oIII* phase transition during the cooling

phase of the crystallization process than the *t*-*m* phase transition, as predicted by the nudged elastic band (NEB) model [20], [21].

Further, excessive doping concentrations or oxygen vacancies are shown to have negative effects on the ferroelectricity of HfO<sub>2</sub>. These conditions were shown to increase the stability of *t*-phase, reducing the likelihood of *t*-*oIII* phase transition during cooling [20], [21]. For instance, the use of reducing electrodes such as TiN or TaN results in oxygen deprivation in the nearby HfO<sub>2</sub> region leading to the formation of *t*-phase next to the electrodes [21], [36]. In addition, first principles simulations have revealed that mechanical stress can significantly affect the phase stabilization and distribution in the HfO<sub>2</sub> thin films. Mechanical stress can result from various factors such as the mechanical confinement of capping layers during crystallization or the polarization induced strain [20], [21].

The ferroelectric *oIII* phase in HfO<sub>2</sub> is characterized by two distinct oxygen sublattices: a centrosymmetric (spacer or non-polar) sublattice and non-centrosymmetric (polar) sub-lattice [9], [19] (Figure 3(a)). The polarization in HfO<sub>2</sub> arises due to the displacement of the non-centrosymmetric oxygen atoms (Figures 1(c) and 3(a)). Several studies have investigated the microscopic configuration of polarization domains and their interaction using first principles calculations. Lee et al. [9] demonstrated that the spacer sublattice separating the polar sublattices in HfO<sub>2</sub> results in flat phonon bands, which renders the dipoles almost independent of one another. Consequently, they proposed that polarization dipoles can be stabilized in laterally ultra-thin domains of sub-nanometer scale in HfO<sub>2</sub>.

Among the various possible  $180^\circ$  and  $90^\circ$  domain walls, the atomically sharp  $180^\circ$  domain walls, composed of alternate polar and non-polar layers in each domain, have been found to be the minimum energy configuration [22] (Figure 3(a)). Interestingly, this type of domain wall has been shown to have slightly negative domain wall energy, making it more energetically favorable than a uniformly polarized single domain state. In this multi-domain configuration, polarization reversal through domain wall motion occurs through the switching of the polar layer, while the polarization in the spacer layer remains fixed.

Apart from the phase stability and microscopic domain configurations, first principles simulations have been employed in studying the effects of dead or interfacial layers [23]. Dead layers are non-ferroelectric layers that are formed at the HZO-metal and HZO-semiconductor interfaces during deposition due to the diffusion of oxygen ions across the interface. These layers result in imperfect screening of the polarization charges at the interface, leading to a significant electric field build up in both the ferroelectric and dead layers. This high field, combined with the bond strains at the interface, induces the formation of oxygen vacancies. These vacancies migrate into the HZO layer with the applied electric field cycling, causing endurance degradation [24], [36].

First principles simulations have been instrumental in understanding the factors contributing to the higher endurance values observed in  $\text{HfO}_2\text{-ZrO}_2$  superlattices. In a recent study by Gong et al. [24], it was shown that  $\text{HfO}_2\text{-ZrO}_2$  superlattices have higher oxygen vacancy migration barriers along the polarization direction compared to HZO. This finding has helped explain the higher endurance of  $\text{HfO}_2\text{-ZrO}_2$  superlattices and highlights the importance of preventing the diffusion of oxygen vacancies from the interface into FE layer in thin films.

However, studying the evolution of polycrystalline structures and the distribution of different phases across the FE layer using first principles simulations are computationally intensive, requiring simulations of large number of unit cells.

To address this challenge, researchers have traditionally utilized second-principles [18], [26] and phase-field models [25], [26]. Second-principles models are based on principles as first-principles simulations in combination with empirical data fitting. Thereby reducing the computational cost and increasing the number of atoms and time scale of simulations [18]. Second-principles simulations have been used to study the phase-transitions around the Curie temperature [18] in ferroelectrics and the distribution of multiple phases [26].

On the other hand, the phase-field models lack atomistic details, they provide insights at the macroscopic level by describing the material's structure through the spatial distribution of order parameters. The spatial and temporal evolution of these order parameters is determined by minimizing a pre-defined total energy function. Krill et al. [25] developed a grain growth model that captures the evolution of polycrystalline structures (Figure 3(b)) in the ferroelectric layer by considering the mobility of grain boundaries and minimizing the surface and bulk energies of the grains. Building on the insights from first principles studies, Chen et al. [26] developed a multi-phase coexistence phase-field model that predicts the distribution of different phases over the ferroelectric layer based on the underlying grain sizes. This model minimizes the overall phase-specific surface and bulk free energies.

To summarize, material-level models using first principles simulations and phase-field models have been essential in understanding the fundamental aspects of ferroelectricity in HZO. They have provided valuable insights into phase stabilization, microscopic domain configurations and their complex interdependencies. Further refinement and enhancement of these models will be crucial in the optimization of  $\text{HfO}_2$  as a ferroelectric material and advancing the field of ferroelectric thin films.

## DEVICE-LEVEL MODELS

To develop and optimize the performance of ferroelectric devices for a variety of applications, it is critical to understand their behavior and dependen-

cies on design parameters. Device-level models capture the polarization switching and other characteristics of ferroelectric devices and correlate them with the underlying physical mechanisms. By integrating the insights on material properties obtained from the material-level models, device-level models provide a comprehensive and reliable means to predict and study the impact of different design parameters on the ferroelectric device performance. Additionally, they facilitate the exploration of potential applications of ferroelectric devices in various fields.

In the past, analytical models based on the polarization switching equations (Section II) were primarily used for modeling ferroelectric devices, along with simpler numerical models such as the Preisach model. These models provided great insights into the physical mechanisms of ferroelectric devices and identified key parameters affecting their performance. However, as the device dimensions shrank and more complex phenomena, such as polycrystalline nature, presence of defects etc. needed to be captured, analytical models have become increasingly complex and less accurate. With the increasing computational power and resources available, numerical methods have currently become the dominant approach to ferroelectric device modeling [27], [28], [29], [30], [31], [32], [33], [34], [35], [36]. Nevertheless, analytical models remain popular for compact or circuit compatible models where speed is of essence [43], [44].

Numerical models of ferroelectric devices typically involve capturing the spatial distribution of polarization in the ferroelectric layer. To capture the electrostatics, these models couple the polarization switching equations with Poisson's equation and other equations such as drift-diffusion and current continuity for transistors (FEFETs) [27], [28], [29], [30], [31], [32], [35], [36] or tunneling current equations (using WKB approximation or NEGF formalism) [33] for ferroelectric tunnel junctions (FJTs). Occasionally, additional equations are included to account for phenomena such as polycrystallinity and

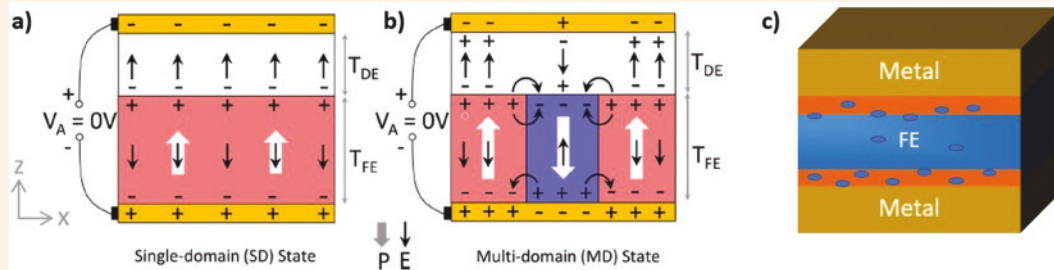


**FIGURE 4** Metal-ferroelectric-insulator-metal (MFIM) stack in (a) single domain polarization state showing the imperfect screening at the FE-DE interface and the depolarization field opposite to the polarization direction in the FE layer and (b) multi-domain polarization state showing reduced depolarization field in the FE layer and the emergence of stray electric fields at the FE-DE interface. (c) MFM stack showing the formation of dead layers at the metal-FE interfaces and high density of defects or O-vacancies in the dead layers.

the presence of defects [34], [35], [36]. Among the various numerical modeling techniques, device models based on TDGL and NLS frameworks are most commonly used for Hafnium-Zirconium-Oxide (HZO) ferroelectric devices. However, the elastic and electro-strictive energies are often neglected in TDGL-based models for non-volatile memories and NCFETs due to their negligible impact and the lack of properly determined coefficients.

When a ferroelectric layer is interfaced with a dielectric, such as in the gate stack of FEFETs, imperfect screening of polarization charges at the interfaces results in the depolarization field (an E-field opposite to the polarization direction) in the FE layer. This leads to an increase in the electrostatic energy ( $E_{elec}$ ), commonly referred to as depolarization energy (Figure 4(a)). As a consequence, FE layer breaks into multiple domains with polarization pointing in the opposite directions alternatively. This multi-domain formation reduces the depolarization energy, as the stray electric fields originating from the  $+P$  domains terminate in the adjacent  $-P$  domains, thereby reducing the electric field in the bulk (Figure 4(b)). However, this comes at the expense of increased gradient energy ( $E_{grad}$ ), due to the domain walls [28]. Multi-domain formation leads to non-uniform electric fields in the ferroelectric layer, which have significant impact on the underlying transistor channel in the FEFETs and the tunneling current in FTJs [27], [28], [29]. Understanding the formation of multi-domain structure as the interplay between

gradient and depolarization energies and its response to the external electric field and device parameters is crucial for optimizing the ferroelectric devices.

Saha et al. [27] developed a self-consistent model for FEFET to account for the interactions between non-uniform polarization in the FE layer and the underlying FET channel. This model couples a 1D TDGL equation (which captures polarization profile along the length of the channel) with Poisson's, NEGF charge and current equations. Using this model, the authors investigated the effect of polarization variation along the gate length. They have shown that the negative drain-induced barrier lowering (DIBL) and negative output conductance in FEFETs arise due to non-monotonic dependence of source barrier on drain voltage. They also studied the dependence of the negative-capacitance effect and the NCFET switching slope on the FE domain interactions [27].

Saha et al. [28] extended their work by developing a 2D TDGL equation-based (capturing polarization profile along the thickness and length of the ferroelectric layer) phase-field model for FEFETs that inherently captures the multi-domain formation. Their study revealed that as ferroelectric thickness ( $T_{FE}$ ) increases, domain density also increases, leading to a decrease in the remanent polarization ( $P_R$ ) of the FE layer, and thereby the memory window of FEFETs. Further, they have demonstrated that higher domain density at lower  $T_{FE}$  favors polarization switching via domain wall motion as opposed to domain nucleation that is dominant at lower

domain densities or higher  $T_{FE}$ . Domain wall motion leads in gradual change in the polarization with the applied voltage at lower  $T_{FE}$ , leading to multi-level memory operations. The authors have also provided insights into the enhanced permittivity observed in ferroelectric layers with thicknesses below 3nm, which is attributed to the transformation of stray E-field from in-plane to out-of-plane direction with increase in applied voltage.

Phase-field models, due to their self-consistent nature, have enabled the study of hard and soft domain walls in HZO and their dependence on  $T_{FE}$  and the gradient energy coefficient [29]. Hard domain walls exhibit abrupt polarization change or high polarization gradient and show hysteretic behavior with voltage cycling. Whereas soft domain walls have low polarization gradients and typically show non-hysteretic behavior. The hysteretic and non-hysteretic negative capacitance (NC) behavior [12] resulting from the domain-wall motion in hard and soft-domain wall regimes has been investigated by Park et al. [30] and Saha et al. [29]. They have studied the dependence of negative capacitance on various design parameters such as applied voltage, ferroelectric and dielectric thickness. Moreover, Saha et al. [29] have showed that the non-uniform electric field in the multi-domain FE layer causes rippling conduction and valence band profiles in the underlying channel of FEFETs, which leads to reduced short channel effects compared to conventional transistors.

Phase-field models are known to inherently capture the formation of



different domain configurations and their dependencies which is crucial in modeling ferroelectric devices. However, they are often computationally intensive, which limits their application mainly to smaller-scale devices. On the other hand, NLS based models offer computationally efficient alternative to simulate the ferroelectric devices. However, these models have limited ability to capture the formation of multi-domains and their dependencies. In NLS models, the multi-domain formation is captured by explicitly dividing the FE layer into multiple independent regions. Moreover, NLS-based models do not explicitly capture the effect of various external perturbations such as temperature and strain. To address these limitations, Pesic et al. [20] developed a ferroelectric device model that combines the ideas of TDGL formalism and NLS frameworks. This model partitions the FE layer into multiple smaller regions, each representing a polarization domain. These regions are governed by a homogeneous or single domain TDGL equation (also known as the Landau-Khalatnikov equation).

In the regime of NLS-based models, Alessandri et al. [31] developed a kinetic Monte Carlo (KMC) simulation framework for FE capacitor. This model addresses the limitations of the original NLS formalism, such as the requirement of initial fully poled polarization state and application of constant electric field. The KMC framework introduces an auxiliary history parameter ( $h^i(t)$ ) for each region to replace the characteristic time constant. This parameter tracks the history of the electric field and polarization state of the region, thereby enabling the model to capture the effects of arbitrary applied electric fields and initial conditions. This framework has been shown to accurately capture the characteristics of FE capacitors with arbitrary voltage pulses, as observed in experiments. Moreover, it also captures the effects of area scaling, predicting a sharp polarization switching in small area samples.

Deng et al. [32] have extended the framework to FEFETs and investigated the impact of area scaling on device-to-device variations. By utilizing the history of switching probabilities of a region,

the authors have shown the ability of the KMC framework to capture the stochastic nature of polarization switching and the accumulation property of the switching probabilities. NLS models have also been instrumental in modeling ferroelectric tunnel junctions (FTJs). Xiao et al. [33] have extended the KMC framework to FTJs by coupling it with the multi-band tunneling current equations based on WKB approximation. Using this model, they have studied the effects of doping, ferroelectric, and interfacial layer thicknesses on the tunneling electro resistance (TER). They have also performed a design space exploration of the FTJs to optimize the write functionality of memory and analog weight cell.

Capturing the polycrystalline and polymorphic nature of HZO along with the presence of defects is crucial to understand the variability and endurance issues of HZO-based ferroelectric devices [10]. NLS models, specifically KMC model, account for polycrystallinity by considering variations in the activation fields ( $E_a$ ) of the regions. These models have predicted an increase in polycrystallinity-induced variations with area scaling due to a reduction in number of domains. To further explore the effects of polycrystallinity, Koduru et al. [34] coupled the TDGL based phase field model [28] with a grain growth model [25]. Their study investigated the impact of thickness scaling in small area devices and showed that the increase in domain density with reducing thickness can help reduce the device-to-device variations in the polarization switching.

Chang et al. [35] have developed a TDGL based phase-field model for FEFETs that captures the coexistence of multiple phases (o-, m- and t-) using Kittel's formalism and accounts for the presence of defects. They have demonstrated that the evolution of the phase distribution in the ferroelectric layer, from t-phase to o-phase to m- phase with field cycling can explain the wake-up and fatigue effects observed in HZO-based devices. In addition, they have also shown that charge trapping in the defects at the interfaces between polar and non-polar phases results in the imprint or the gradual shift in the P-E characteristics of the device.

To study in depth the influence of field cycling, Pesic et al. [36] have developed a comprehensive modeling approach for HZO-based devices. This model captures the oxygen vacancy and defect generation, recombination, and transport mechanisms. The authors demonstrated that the interfacial oxide layers (dead layers) contain high density of defects or oxygen vacancies, which diffuse into the HZO layer with field cycling. This diffusion of oxygen vacancies into the ferroelectric layer is the primary cause of the t- to o-phase transformation. This transformation leads to an initial increase in the polarization, known as the wake-up effect. Further, these interfacial oxide layers experience very high depolarization fields due to imperfect screening of polarization charges. The authors have shown that constant switching of these high fields due to applied electric field cycling results in the breakage of oxygen bonds in the interfacial layer, generating more defects (Figure 4(c)). As the number of defects in the interfacial layer and the trapping of charges by these defects increases, the electric field experienced by the ferroelectric layer reduces. This impedes the switching of the domains in ferroelectric layer, leading to domain pinning. This reduces the number of domains available for switching for a given applied electric field, resulting in a decrease in the polarization, as seen in the fatigue stage [36].

In conclusion, device-level models have been valuable in correlating device performances with the complex physical mechanisms. They have provided great insights into the limitations of FE devices and the underlying mechanisms. However, the calibration of model parameters with experimental results remains time-consuming process. Additionally, as devices continue to shrink, the realistic capture of domain walls and grain boundaries becomes increasingly important, as well as the development of models for emerging HfO<sub>2</sub> based superlattice heterostructures. To drive the advancement and optimization of ferroelectric devices for a wide range of applications, the continued development of device-level models that capture these nuances will be crucial.

## COMPACT OR CIRCUIT-COMPATIBLE MODELS

Design and evaluation of circuits using FE devices for a variety of applications [7] rely on the development of precise and computationally efficient models. Circuit compatible or compact models are typically developed based on the insights from device-level models. These models enable the analysis of the effects of material and device parameters on circuit behavior. By accurately capturing and predicting the characteristics of ferroelectric devices, circuit-compatible models help test the circuit functionality and optimize performance.

In the early stages of ferroelectric compact modeling, several models based on Preisach theory and Miller's equations were proposed to capture the hysteretic polarization switching [17], [18], [43], [44]. However, with the proposal of NCFETs in 2008 [13], there were several attempts to develop circuit-compatible models based on Landau formalism. One such model was proposed by Aziz et al. [37], which models the FE layer of FEFET entirely in SPICE using equivalent circuit elements for the LK equation. The non-linear part of the equation is modeled via a feedback circuit using behavioral description of SPICE circuit elements. The overall representation of the FE layer included the non-linear capacitor in series with a resistor to model the delay, along with other capacitors that model the non-ideal effects of FE layer and contacts. The FE layer is self-consistently coupled with the gate terminal of a MOSFET to model the FEFET. Using this model, the authors have captured the NCFET functionality and analyzed its applications.

Another compact model for FEFET was developed in Verilog-A by Alam et al. [38], where the LK equation is integrated with the MIT Virtual Source (MVS) transistor model. Further, Duarte et al. [39] developed distributed charge and lumped charge models for FEFETs, based on the LK equation for FE layer and BSIM-CMG model for the underlying MOSFET. These models capture the distributed nature of the FE device by evaluating the charge and voltage along the channel length. Using these models, the authors captured the NC effect and

investigated the impact of ferroelectric thickness, gate and drain voltages on the subthreshold switching slope.

To capture the formation of multi-domain structure in the FE layer, Asai et al. [40] proposed a compact model for FEFET by dividing the FE layer into multiple capacitors. Each of the capacitors is modeled using the single-domain LK equation and is assumed to be independent in its switching. The effect of the FE layer on the underlying oxide capacitance was considered as the collective effect of all the FE capacitors in parallel. Although this model captures the non-homogeneous nature of polarization in the FE layer, the effect of the resultant non-homogeneous electric field on the underlying FET is not captured. To address this, Gaidhane et al. [41] developed a compact model for FEFET in which the underlying FET was also divided into multiple FETs connected as a 2D array between the source and the drain terminals, each with its own FE capacitor. This model is able to capture the interactions between the non-uniform electric field and the underlying transistor but tends to be computationally intensive.

To capture the effects of polycrystallinity, Pesic and Hoffmann et al. [21] proposed a modified LK based approach in which the FE layer is divided into multiple smaller regions in parallel, representing the grains of polycrystalline structure. In this model, each grain is assumed to be governed by a single domain LK equation, represented using a non-linear capacitor in series with a resistor and a voltage source emulating the internal bias fields. To capture variations across the grains, the authors considered distributions in the parameters governing the non-linear capacitor. Additionally, the possible dielectric nature of some of the grains was captured using a linear capacitor in parallel. Further, Tung et al. [42] developed an analytical model for FEFETs by dividing the FE layer into a group of grains or regions. The authors proposed an analytical equation to capture the polarization switching in each region, which is dependent on the area fraction of the grain that is unswitched and on a time constant that tracks the history of the electric field in the region, similar to Kinetic Monte Carlo (KMC) framework. This model is able to capture the effects

of polycrystallinity and the impact of area scaling on the device performance.

Ni et al. [43] proposed a compact model that couples the Preisach theory of hysteresis (via Miller's equations) and history tracking, along with RC type delay elements. The authors demonstrated the model's ability to capture the arbitrary waveforms for applied voltage and investigated the impact of applied voltage pulses on the binary and analog memory characteristics of FEFET. Further, Saha et al. [44] utilized a similar model to explore NCFETs. They have explained that the transient negative capacitance observed in FEFETs is due to the delay between the polarization switching and the charge compensation.

To accurately evaluate performance of ferroelectric devices, it is crucial to take into account the trapping effects in the compact models. Trapping of electrons or holes by the defects reduces the number of ferroelectric domains available for switching resulting in a reduction of memory window of FEFET [36]. This effect can be captured by considering an auxiliary voltage source in the gate stack of FEFET, which reduces the effective voltage across the FE layer, as demonstrated in [20]. Further, Xiang et al. [45] developed a compact model that captures the effects of charge trapping in multi-domain FEFETs by considering nucleation-growth domain reversal dynamics coupled with charge trapping model.

Researchers have made significant progress in developing circuit-compatible models that accurately capture the performance of ferroelectric devices and their dependencies on design parameters. These models had aided in the design and optimization of ferroelectric-based circuits, and enabled the exploration of various potential applications. However, most of these models consider the lump effect of the ferroelectric layer on the underlying FET. As the demand for high-performance circuits continues to grow, there is an urgent need to develop models that can effectively capture the distributed nature of FE devices, along with multi-domain and polycrystalline effects. These models will aid in accurately modeling the performance of FE devices and its dependence on design parameters.

## SUMMARY

In this article, we discussed different modeling frameworks for ferroelectric devices, covering material, device, and circuit levels. We have highlighted the importance of material-level models in the understanding of underlying aspects of ferroelectric material and their crucial role in driving the material optimization. At the device level, we have discussed various models that capture the characteristics of FEFETs and their role in correlating the device performance to underlying physical mechanisms. We have emphasized the need for self-consistent models that accurately capture device performance and its dependencies for commercialization purposes. Finally, we have discussed the importance of circuit-compatible models for the design and optimization of ferroelectric-based circuits for various applications.

## ACKNOWLEDGMENTS

This work was supported by SRC under Grant 2020-LMD-2959 and by NSF under Grant 2008412.

## ABOUT THE AUTHORS

**Revanth Koduru** (corresponding author: (kodurur@purdue.edu)) is with the Elmore Family School of Electrical and Computer Engineering, Purdue University, West Lafayette, IN, 47907, USA.

**Tanmoy Kumar Paul** (paul115@purdue.edu) is with the Elmore Family School of Electrical and Computer Engineering, Purdue University, West Lafayette, IN, 47907, USA.

**Sumeet Kumar Gupta** (guptask@purdue.edu) is with the Elmore Family School of Electrical and Computer Engineering, Purdue University, West Lafayette, IN, 47907, USA.

## REFERENCES

- [1] J. Valasek, "Piezoelectric and allied phenomena in Rochelle salt," *Phys. Rev.*, vol. 17, no. 4, pp. 475–481, 1921.
- [2] A. von Hippel, "High dielectric constant ceramics," *Ind. Eng. Chem.*, vol. 38, no. 11, pp. 1097–1109, 1946.
- [3] J. F. Scott, "Applications of modern ferroelectrics," *Science*, vol. 315, no. 5814, pp. 954–959, 2007.
- [4] A. F. Devonshire, "XCVI. Theory of barium titanate: Part I," *London, Edinburgh, Dublin Philos. Mag. J. Sci.*, vol. 40, no. 309, pp. 1040–1063, 1949.
- [5] S.-Y. Wu, "A new ferroelectric memory device, metal-ferroelectric-semiconductor transistor," *IEEE Trans. Electron Devices*, vol. 21, no. 8, pp. 499–504, Aug. 1974.
- [6] L. Esaki et al., "Polar switch," *IBM Tech. Discl. Bull.*, vol. 3, no. 2161, p. 114, 1971.
- [7] U. Schroeder et al., "The fundamentals and applications of ferroelectric HfO<sub>2</sub>," *Nature Rev. Mater.*, vol. 7, no. 8, pp. 653–669, 2022.
- [8] T. S. Boscke et al., "Ferroelectricity in hafnium oxide thin films," *Appl. Phys. Lett.*, vol. 99, no. 10, 2011, Art. no. 102903.
- [9] H. J. Lee et al., "Scale-free ferroelectricity induced by flat phonon bands in HfO<sub>2</sub>," *Science*, vol. 369, no. 6509, pp. 1343–1347, 2020.
- [10] M. Pešić and B. Beltrando, "Embedding ferroelectric HfO<sub>x</sub> in memory hierarchy: Material-defects-device entanglement," in *Proc. IEEE Int. Electron Device Meeting*, 2021, pp. 33.4.1–33.4.4.
- [11] V. L. Ginzburg, "Second-order phase transitions," *Sov. Phys. Solid State*, vol. 2, p. 1123, 1960.
- [12] A. M. Bratkovsky and A. P. Levanyuk, "Depolarizing field and 'real' hysteresis loops in nanometer-scale ferroelectric films," *Appl. Phys. Lett.*, vol. 89, no. 25, 2006, Art. no. 253108.
- [13] S. Salahuddin and S. Datta, "Use of negative capacitance to provide voltage amplification for low power nanoscale devices," *Nano Lett.*, vol. 8, no. 2, pp. 405–410, 2008.
- [14] Y. Ishibashi and T. Yutaka, "Note on ferroelectric domain switching," *J. Phys. Soc. Jpn.*, vol. 31, no. 2, pp. 506–510, 1971.
- [15] A. K. Tagantsev et al., "Non-Kolmogorov-Avrami switching kinetics in ferroelectric thin films," *Phys. Rev. B*, vol. 66, no. 21, 2002, Art. no. 214109.
- [16] A. T. Bartic et al., "Preisach model for the simulation of ferroelectric capacitors," *J. Appl. Phys.*, vol. 89, no. 6, pp. 3420–3425, 2001.
- [17] S. L. Miller et al., "Modeling ferroelectric capacitor switching with asymmetric nonperiodic input signals and arbitrary initial conditions," *J. Appl. Phys.*, vol. 70, no. 5, pp. 2849–2860, 1991.
- [18] P. Ghosez and J. Junquera, "Modeling of ferroelectric oxide perovskites: From first to second principles," *Annu. Rev. Condens. Matter Phys.*, vol. 13, pp. 325–364, 2022.
- [19] R. Materlik et al., "The origin of ferroelectricity in Hf<sub>1-x</sub>Zr<sub>x</sub>O<sub>2</sub>: A computational investigation and a surface energy model," *J. Appl. Phys.*, vol. 117, no. 3, 2015, Art. no. 134109.
- [20] M. Pestic et al., "A computational study of hafnia-based ferroelectric memories: From ab initio via physical modeling to circuit models of ferroelectric device," *J. Comput. Electron.*, vol. 16, pp. 1235–1256, 2017.
- [21] M. H. Park et al., "Ferroelectricity and antiferroelectricity of doped thin HfO<sub>2</sub>-based films," *Adv. Mater.*, vol. 27, no. 11, pp. 1811–1831, 2015.
- [22] W. Ding et al., "The atomic-scale domain wall structure and motion in HfO<sub>2</sub>-based ferroelectrics: A first-principles study," *Acta Materialia*, vol. 196, 2020, Art. no. 556.
- [23] K. Chae et al., "Hafnium-zirconium oxide interface models with a semiconductor and metal for ferroelectric devices," *Nanoscale Adv.*, vol. 3, no. 16, pp. 4750–4755, 2021.
- [24] Z. Gong et al., "Physical origin of the endurance improvement for HfO<sub>2</sub>-ZrO<sub>2</sub> superlattice ferroelectric film," *Appl. Phys. Lett.*, vol. 121, 2022, Art. no. 242901.
- [25] C. E. Krill III et al., "Computer simulation of 3-D grain growth using a phase-field model," *Acta Materialia*, vol. 50, no. 12, pp. 3059–3075, 2002.
- [26] Q. Chen et al., "Ferroelectric switching behavior of nanoscale Hf<sub>0.5</sub>Zr<sub>0.5</sub>O<sub>2</sub> grains," *Int. J. Mech. Sci.*, vol. 212, 2021, Art. no. 106828.
- [27] A. K. Saha, P. Sharma, I. Dabo, S. Datta, and S. K. Gupta, "Ferroelectric transistor model based on self-consistent solution of 2D Poisson's, non-equilibrium Green's function and multi-domain Landau Khalatnikov equation," in *Proc. IEEE Int. Electron Devices Meeting*, 2017, pp. 13.5.1–13.5.4.
- [28] A. K. Saha, M. Si, K. Ni, S. Datta, P. D. Ye, and S. K. Gupta, "Ferroelectric thickness dependent domain interactions in FEFETs for memory and logic: A phase-field model based analysis," in *Proc. IEEE Int. Electron Devices Meeting*, 2020, pp. 4.3.1–4.3.4.
- [29] A. K. Saha and S. K. Gupta, "Multi-domain negative capacitance effects in metal-ferroelectric-insulator-semiconductor/metal stacks: A phase-field simulation based study," *Sci. Rep.*, vol. 10, no. 1, 2020, Art. no. 10207.
- [30] H. W. Park et al., "Modeling of negative capacitance ferroelectric thin films," *Adv. Mater.*, vol. 31, no. 32, 2019, Art. no. 1805266.
- [31] C. Alessandri, P. Pandey, A. Abusleme, and A. Seabaugh, "Monte Carlo simulation of switching dynamics in polycrystalline ferroelectric capacitors," *IEEE Trans. Electron Devices*, vol. 66, no. 8, pp. 3527–3534, Aug. 2019.
- [32] S. Deng et al., "A comprehensive model for ferroelectric FET capturing the key behaviors: Scalability, variation, stochasticity and accumulation," in *Proc. IEEE Symp. VLSI Technol.*, 2020, pp. 1–2.
- [33] Y. Xiao, S. Deng, Z. Zhao, V. Narayanan, and K. Ni, "Predictive modeling of ferroelectric tunnel junctions for memory and analog weight cell applications," in *Proc. IEEE Int. Electron Devices Meeting*, 2021, pp. 15.5.1–15.5.4.
- [34] R. Koduru, A. K. Saha, M. Si, X. Lyu, P. D. Ye, and S. K. Gupta, "Variation and stochasticity in polycrystalline HZO based MFIM: Grain-growth coupled 3D phase field model-based analysis," in *Proc. IEEE Int. Electron Devices Meeting*, 2021, pp. 15.2.1–15.2.4.
- [35] S.-C. Chang et al., "Multi-domain phase-field modeling of polycrystalline hafnia-based (Anti-) ferroelectric capable of representing defects, wake-up and fatigue," in *Proc. IEEE Int. Electron Devices Meeting*, 2022, pp. 13.1.1–13.1.4.
- [36] M. Pestic et al., "Physical mechanisms behind the field-cycling behavior of HfO<sub>2</sub> based ferroelectric capacitors," *Adv. Funct. Mater.*, vol. 26, no. 25, pp. 4601–4612, 2016.
- [37] A. Aziz, S. Ghosh, S. Datta, and S. K. Gupta, "Physics-based circuit-compatible SPICE model for ferroelectric transistors," *IEEE Electron Device Lett.*, vol. 37, no. 6, pp. 805–808, Jun. 2016.
- [38] M. A. Alam, P. Dak, M. A. Wahab, and X. Sun, "Physics-based compact models for insulated-gate field-effect biosensors, landau-transistors, and thin-film solar cells," in *Proc. IEEE Custom Integr. Circuits Conf.*, 2015, pp. 1–8.
- [39] J. P. Duarte et al., "Compact models of negative-capacitance FinFETs: Lumped and distributed charge models," in *Proc. IEEE Int. Devices Meeting*, 2016, pp. 30.5.1–30.5.4.
- [40] H. Asai et al., "Compact model of ferroelectric-gate field-effect transistor for circuit simulation based on multidomain landau-khalatnikov theory," *Japanese J. Appl. Phys.*, vol. 56, no. 4S, 2017, Art. no. 04CE07.
- [41] A. D. Gaidhane et al., "Study of multi-domain switching dynamics in negative capacitance FET using SPICE simulations," *Microelectronics J.*, vol. 115, 2021, Art. no. 105186.
- [42] C.-T. Tung, G. Pahwa, S. Salahuddin, and C. Hu, "A compact model of polycrystalline ferroelectric capacitor," *IEEE Trans. Electron Devices*, vol. 68, no. 10, pp. 5311–5314, Oct. 2021.
- [43] K. Ni, M. Jerry, J. A. Smith, and S. Datta, "A circuit compatible accurate compact model for ferroelectric-FETs," in *Proc. IEEE Symp. VLSI Technol.*, 2018, pp. 131–132.
- [44] A. K. Saha et al., "Negative capacitance in resistor-ferroelectric and ferroelectric-dielectric networks: Apparent or intrinsic?," *J. Appl. Phys.*, vol. 123, no. 10, 2018, Art. no. 105102.
- [45] Y. Xiang et al., "Compact modeling of multi-domain ferroelectric FETs: Charge trapping, channel percolation, and nucleation-growth domain dynamics," *IEEE Trans. Electron Devices*, vol. 68, no. 4, pp. 2107–2115, Apr. 2021.